ATMOSPHERE, IONOSPHERE, SAFETY

Part 1

Kaliningrad
2018

IMMANUEL KANT BALTIC FEDERAL UNIVERSITY
SEMENOV INSTITUTE OF CHEMICAL PHYSICS, RAS
PUSHKOV INSTITUTE OF TERRESTRIAL MAGNETISM, IONOSPHERE
AND RADIO WAVE PROPAGATION, RAS

ATMOSPHERE, IONOSPHERE, SAFETY

Proceedings
of VI International conference

Part 1

Kaliningrad
2018

UDK 550.51
BBK 552.44
A92

The conference AIS-2018 was supported by Russian Foundation for Basic Researches (Grant No. 18-03-20020); the VarSITI program and the program «5-100» for improving competitiveness at Immanuel Kant Baltic Federal University.

A92 **Atmosphere, ionosphere, safety** / edited by I.V. Karpov, O.P. Borchevkina. — Kaliningrad, 2018. — Pt. 1 — 360 p.
ISBN 978-5-9971-0490-0 (Pt. 1)
ISBN 978-5-9971-0491-7

Proceedings of International Conference "Atmosphere, ionosphere, safety" (AIS-2018) include materials reports on: (1) — response analysis of the atmosphere — ionosphere to natural and manmade processes, various causes related geophysical phenomena and evaluate possible consequences of their effects on the human system and process; (2) — to study the possibility of monitoring and finding ways to reduce risk. Scientists from different countries and regions of Russia participated in the conference. Attention was given to questions interconnected with modern nanotechnology and environmental protection. Knowledge of the factors influencing the atmosphere and ionosphere can use them to monitor natural disasters and to establish the appropriate methods on this basis.

Content of the reports is of interest for research and students specializing in physics and chemistry of the atmosphere and ionosphere.

UDK 550.51
BBK 552.44

ISBN 978-5-9971-0490-0 (Pt. 1)
ISBN 978-5-9971-0491-7

2. A. J. Mannucci, B. D. Wilson, D. N. Yuan et al., A global mapping technique for GPS derived ionosphere TEC measurements, *Radio Sci.,* 1998, 33(3), pp. 565—582.

3. A. D. Akchurin, V. V. Bochkarev, V. R. Ildiryakov, and K. M. Usupov, TID selection and research of its characteristics on ionograms, *in 30th URSI on General Assembly and Scientific Symposium*, IEEE, Istanbul, Turk, 2011, p. GP1.23.

Seasonal and Interannual Variability of Temperature and Gravity Wave Intensity from Hydroxyl Emission Observations in Alma Aty

Andrey A. Popov[1], Nikolai M. Gavrilov[1], Alexey B. Andreev[2], and Alexander I. Pogoreltsev[3]

[1]Saint-Petersburg State University, Department of atmospheric physics, Saint Petersburg, Russia, 198504
[2]Science Center KIT, "Institute for Ionosphere", Almaty, plateau Kamenskoye, Kazakhstan, 050020
[3]Russian State Hydrometeorological University, Department of meteorological forecasts, Saint-Petersburg, Voronezhskaya Str., 98

Introduction. Currently, the study of internal gravity wave (IGW) studies are of interest. Their sources are located mainly in the lower atmosphere and, propagating upwards, IGWs are able to transfer energy and momentum to the middle and upper atmosphere, thus influencing the thermodynamic regime of the atmosphere.

Measurements of intensity and rotational temperatures of nightglows is a way for monitoring the dynamics and composition of the upper atmosphere. Authors [1] studied temperature variability in the mesopause region using spectral observations of hydroxyl emission at the Zvenigorod station. The problem of changes in the mesopause region during sudden stratospheric warming was analyzed in [2]. The study [3] deals with seasonal changes of temperature obtained from hydroxyl emission observations and their dependence on solar activity.

Recent studies reveal the presence of long-term changes of the upper atmosphere characteristics [e. g., 4]. Authors [5] used a simple differential filters and analyzed seasonal and interannual changes in the mean winds and IGW intensity at altitudes 80—100 km from observations of the ionospheric drifts at Collm Observatory in Germany.

In this paper, the method of digital differential filtering is applied for analyzing observations of the rotational temperature hydroxyl nightglows at altitudes of 85—90 km with the SATI devise in Alma-Aty, Kazakhstan in years 2010—2017. We study seasonal and interannual changes in the average temperature and in the intensity of variations with periods 1.7—5 hours, which may be associated with IGWs in the mesopause region.

The device and method of data analysis. Information about hydroxyl nightglow at altitudes of 85—90 km is obtained at the Institute of Ionosphere in Alma-Aty, Republic of Kazakhstan. The device SATI (Spectral Airglow

Temperature Imager) is installed at the foothills of the Tien Shan mountain region. The SATI is a Fabry-Perot spectrometer, which uses narrow-band interference filters and a CCD camera detector. The SATI can variations of the intensity and rotational temperature in the bands of OH emission. To select them, the SATI uses interference filters for the spectral region of the OH Meinel bands [6]. The exposure time is 2 minutes. The use of the SATI for IGW studies ~~of~~ in the lower thermosphere is described in detail in [7].

The SATI measures the intensity and vibrational temperature of OH emission at the average altitude of 87 km at 12 sky points along almucantar with a zenith angle of 30°. During primary processing, measured values are averaged over all 12 sky points and over hourly time intervals.

To estimate the intensity of short-period perturbations near the mesopause, we used the method described in [5]. To obtain variations with mesoscale time periods, a numerical filtering was applied by calculating the difference between consecutive hourly average values of temperature

$$T'_i = (T_{i+1} - T_i)/2, \tag{1}$$

where i is the number of hourly interval with the middle time t_i. It is shown in [5] that the difference between the average hourly values is equivalent to a numerical frequency filter having the transmission function

$$H^2 = \frac{\sin^4(\sigma\tau/2)}{(\sigma\tau/2)^2}, \tag{2}$$

where σ is frequency, $\tau = t_{i+1} - t_i$ is the time step of the hourly data. Figure 1 shows the transmission function of the filter (2) for τ = 1h. The H^2 maximum in Fig. 1 corresponds to the period about 2.7 h and the half-width of H^2 at the level of 0.5 of the maximum value gives the filtered period interval of 1.7—5.1 h.

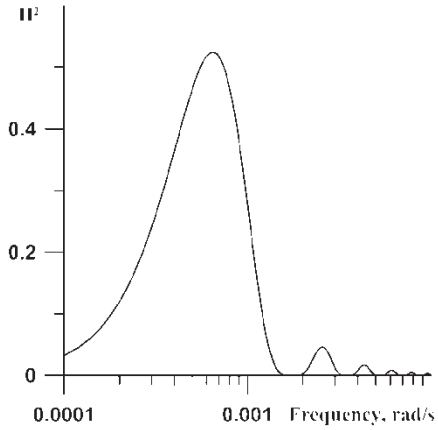

FIGURE 1. Transmission Function of the hourly-difference filter (2).

To improve statistical reliability of results, the filter (2) was applied only to pairs of hourly intervals with at least 40 individual temperature measurements. To study the seasonal and inter-annual changes, the mean temperatures and relative variances of the hourly differences (2) over monthly intervals were calculated.

Results. The method described previously was applied to the data of ground-based observations of the rotational temperature of the OH band (6—2) with the SATI device in Alma-Aty during the interval from May 2010 to April 2017. The polarization relations of the theory of atmospheric IGW [8] allow to obtain the following formula for the amplitude of horizontal velocity variations, U, and potential wave energy, E_p:

$$U = \frac{g}{N}\sqrt{\frac{T'^2}{T_0^2}}; \qquad E_p = \frac{U^2}{2}, \tag{3}$$

where g is the gravitational acceleration, N is the Brund-Vaisala frequency, T_0 is the montly-mean temperature.

Figure 2 shows seasonal changes of the analyzed parameters averaged over years 2010—2017. The mean temperature near the mesopause in Fig. 2a has a maximum in winter and minimum in June. The intensity of mesoscale temperature variations in Fig. 2b and IGW characteristics in Figs. 2c and 2d. have maxima in spring and autumn, also minima in winter and summer. Similar seasonal variations of IGW intensity were obtained from medium-frequency radar observations of winds at altitudes of 80—100 km [9].

Figure 3 presents interannual changes of the analyzed characteristics between years 2010 and 2017. The monthly-mean temperature near the mesopause in Fig. 3a demonstrates quasi-sinusoidal changes in accordance with seasonal changes shown in Fig. 2a. The thin line in Fig. 3a shows the linear regression with parameters presented in the first line of Table 1. The slope of the regression line in Fig. 3a corresponds to the rate of temperature decrease near the mesopause about 20±10 K/decade. This is significantly higher than temperature trends in at altitudes of 80—100 km determined from satellite and other ground-based measurements [e. g., 4]. A reason for the differences could be possible long-term changes in the SATI characteristics.

Figures 3b—3d show interannual changes in the characteristics of mesoscale variations with periods of 1.7—5 h. These changes do not show such expressed quasi-sinusoidal behavior as the mean temperature in Fig. 3a. This is due to the more complex seasonal variations of IGW characteristics having two maxima and two minima in Figs. 2b—2d and their instability in different years. Thin lines in Figs. 3b—3d show linear regression of analyzed values, and parameters are presented in Table 1. The slopes of the regression lines in Figs. 3b—3d correspond to increasing intensity of mesoscale perturbations near the mesopause. Similar positive multi-year trends in IGW intensity were obtained in [10].

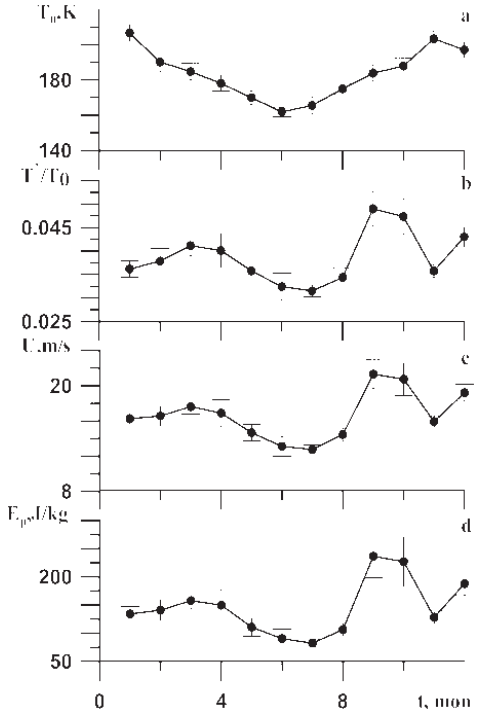

FIGURE 2. Seasonal variations of temperature (a), relative hourly-difference temperature variance (b), amplitude of horizontal velocity perturbation (c) and potential wave energy (d) averaged over years 2010—2017.

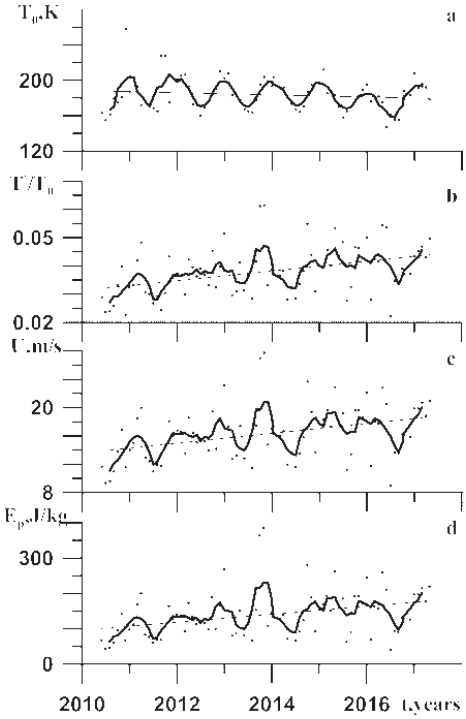

FIGURE 3. Interannual changes of the monthly-mean temperature (a), relative temperature variance (b), amplitude of horizontal velocity perturbations (c), potential wave energy (d). Thin lines shows linear fits.

TABLE 1. Coefficients of multy-year regression lines expressed in the form of $f=a_0+a_1(t-t_0)/10$ for characteristics shown in Fig. 3. Here t is time in years, $t_0 = 2010$.

Parameter	a_1	a_0
T_0	-20±10 Kdec^{-1}	200±100 K
$\lvert T`/T_0 \rvert$	0.017±0.004 dec^{-1}	0.06±0.01
U	6±2 ms^{-1}dec^{-1}	13±4 ms^{-1}
E_p	110±30 J kg^{-1}dec^{-1}	80±30 J kg^{-1}

Conclusion. The method of digital differential filters (2) is applied to the analysis of observations of the rotational temperature of hydroxyl nightglow at altitudes of 85—90 km with the SATI device in Alma-Aty, Kazakhstan in years

2010—2017. Analyzed are interannual and seasonal changes in the monthly-mean temperature and characteristics of temperature perturbations with mesoscale periods, which may be associated with IGW in the mesopause region. To obtain variations with time periods of 1.7—5 h a numerical filtering was used by calculating the differences between consecutive hourly-mean temperature values. The mean temperature near the mesopause has a maximum in winter and minimum in June. IGW intensities maximize in spring and autumn and minimize in winter and summer. The slopes of regression lines in Figs. 3b—3d correspond to multi-year increasing intensity of mesoscale perturbations near the mesopause.

This study was supported by the Russian Basic Research Foundation (#17-05-00458).

1. V. I. Perminov, A. I. Semenov, I. V. Medvedeva, and N. N. Pertsev, The temperature change in the area of the mesopause by observation of hydroxyl emission in the mid-latitudes, *Geomagn. Aeron.*, 2014, 54(2), pp. 230—239.

2. I. V. Medvedeva, A. B. Beletskii, V. I. Perminov et al., Variations in atmospheric temperature at heights of the mesopause and lower thermosphere during periods of stratospheric warming, according to ground and satellite measurements in different longitude sectors, *Sovremennyye problemy distantsionnogo zondirovaniya Zemli iz kosmosa*, 2011, 8(4), pp. 127—135 (in Russian).

3. A. M. Ammosova and P. P. Ammosov, Seasonal variations of temperature and emission intensities of mesopause on variation of solar activity, *Proceeding of SPIE, Eighteenth International Symposium on: Atmospheric and Ocean Optics/Atmospheric Physics*, 2012, 8696, 86960S, doi: 10.1117/12.2008792.

4. J. Lastovichka, A review of recent progress in trends in the upper atmosphere, *J. Atmos. Sol.-Terr. Phys*., 2017, 163, pp. 2—13.

5. N. M. Gavrilov, C. Jacobi, and N. Kurshcner, Drifts and their short-period perturbations in the lower ionosphere observed at Collm during 1983 — 1999, *Phys. Chem. Earth*, *Part C: Sol.-Terr. Planet. Sci.*, 2002, 26, pp. 459—464.

6. M. J. Lopez-Gonzalez, E. Rodrıguez, R. H. Wiens et al., Seasonal variations of O2 atmospheric and OH(6–2) airglow and temperature at mid-latitudes from SATI observations, *J. Atmos. Sol.-Terr. Phys*., 2007, 69, pp. 2379—2390.

7. R. H. Wiens, A. Moise, S. Brown et al., SATI: A spectral airglow temperature imager, *Adv. Space Res.*, 1997, 19, pp. 677—680.

8. E. E. Gossard and W. H. Hook, *Waves in atmosphere*, 1978, M.: Mir, 530 p.

9. N. M. Gavrilov, D. M. Riggin, and D. C. Fritts, Medium-frequency radar studies of gravity-wave seasonal variations over Hawaii (22°N, 160°W), *J. Geophys. Res*., 2003, 108(D20), 4655, doi:10.1029/2002JD003131.

10. N. M. Gavrilov, S. Fukao, T. Nakamura et al., Comparative study of interannual changes of the mean winds and gravity wave activity in the middle atmosphere over Japan, Central Europe and Canada, *J. Atmos. Sol.-Terr. Phys*., 2002, 64, pp. 1003—1010.